Towards Bayesian Parameter Estimation For The Post-Merger Gravitational Wave Signal In Binary Neutron Star Coalescence

J. Clark[1]

[1] *University of Massachusetts Amherst, Amherst, MA 01003, USA*

(Dated: July 24, 2014)

Some notes & preliminary results for Bayesian post-merger analysis. So far, we have the ability to compute matches (time- and phase-maximised overlap) between numerical post-merger signals and a simple template. This part also estimates the expected bias in the recovery of f_2. Finally, we have preliminary estimates of f_2 measurability for optimally oriented signals in a single detector as a function of distance for the DD2 (1.35+1.35) waveform using a parallel-tempering MCMC algorithm with the aforementioned templates. The goal at this point is to extend these results to a few different waveforms and then perform a small demonstration of combining the measurements, in a coherent Bayesian manner, from multiple post-merger signals for a single EOS with slightly different binary masses.

PACS numbers: 04.80.Nn, 07.05.Kf, 97.60.Jd, 04.25.dk

I. INTRODUCTION

II. AD HOC TEMPLATES

From visual inspection of the post-merger waveforms (as well as from more detailed spectral analysis) one is immediately inclined to suspect that a simple, monochromatic damped-sinusoid may be sufficient to recover the peak frequency (f_2) using a matched-filter analysis. However, closer inspection of the spectral content reveals that the dominant post-merger oscillation peak is closer to a Gaussian, rather than a Lorentzian. Furthermore, there is often a slight asymmetry in the post-merger peak arising from the non-stationarity of the instantaneous frequency over the evolution of the post-merger remnant. While it is tempting to try to model the frequency evolution based on numerical simulations, such a template will necessarily introduce a large number of parameters, complicating the data analysis. Here, we will consider the expected performance of four very simple analytical prescriptions for the post-merger signal:

Exponentially-damped Sinusoid ('Ring-down', RD):

$$h_{RD}(t-t_0) = \begin{cases} A_0 \sin(2\pi f_0 t + \phi_0) e^{-\frac{t}{2\tau}} \text{ for } t \geq t_0 \\ 0 \text{ otherwise.} \end{cases} \tag{1}$$

Gaussian-damped Sinusoid ('Gauss-down', GD):

$$h_{GD}(t-t_0) = \begin{cases} A_0 \sin(2\pi f_0 t + \phi_0) e^{-\frac{t^2}{2\tau^2}} \text{ for } t \geq t_0 \\ 0 \text{ otherwise.} \end{cases} \tag{2}$$

Exponentially-damped Chirp ('Chirping Ring-down', CRD): We now allow the phase of the sinusoidal part of the waveform to evolve such that the frequency increases linearly in time:

$$h_{RC}(t-t_0) = \begin{cases} A_0 \sin(2\pi f_0 t + \phi(t) + \phi_0) e^{-\frac{t}{2\tau}} \text{ for } t \geq t_0 \\ 0 \text{ otherwise,} \end{cases} \tag{3}$$

where the phase evolution is given by,

$$\phi(t) = \text{Look this up } \ldots. \tag{4}$$

Gaussian-damped Chirp ('Chirping Gauss-down', CGD): We now allow the phase of the sinusoidal part of the waveform to evolve linearly in time:

$$h_{GC}(t-t_0) = \begin{cases} A_0 \sin(2\pi f_0 t + \phi(t) + \phi_0) e^{-\frac{t^2}{2\tau^2}} \text{ for } t \geq t_0 \\ 0 \text{ otherwise,} \end{cases} \tag{5}$$

where the phase evolution is again given by equation 4.

In the case of the ring-down and the Gauss-down, the center frequency f_0 is our estimator for f_2 (i.e., the post-merger peak frequency of interest). For the chirping signals, our estimator for f_2 is based on the *average* frequency content of the damped-chirp (the section below will elucidate this point). In the current code-setup, we are able to recover the joint posterior probability density function on the initial frequency and the total change in frequency over the full duration of the waveform. I still need to make sure I understand how to get to the desired estimator for f_2 from these measured parameters.

A. Expected Template Performance: Match & Frequency Bias

Our predictions of templates' relative performance are based on the match; the overlap σ between a numerical waveform $d(t)$ and the template $h(t)$, maximised over all waveform parameters:

$$\sigma = \frac{(d|h)}{\sqrt{(h|h).(d|d)}}, \tag{6}$$

Waveform	Max Broadband Match				Max Narrow-band Match				Bias [Hz]			
	RD	GD	CRD	CSG	RD	GD	CRD	CGD	RD	GD	CRD	CGD
APR	0.254	0.252	0.271	0.268	0.899	0.916	0.983	0.986	20.18	24.18	16.18	12.18
DD2	0.558	0.559	0.561	0.560	0.991	0.991	0.990	0.998	5.08	5.08	-6.92	-0.92
$DD2_{3.3}$	0.273	0.273	0.273	0.273	0.959	0.967	0.996	0.996	-7.36	-9.36	-5.36	-15.36
NL3	0.605	0.605	0.643	0.637	0.923	0.938	0.993	0.997	-11.06	-11.06	-3.06	-3.06
$NL3_{3.8}$	0.399	0.406	0.447	0.445	0.891	0.913	0.971	0.986	-22.93	-22.93	-20.93	-16.93
SFHo	0.320	0.316	0.323	0.312	0.955	0.972	0.999	0.999	6.40	8.40	-11.60	-3.60
SFHx	0.430	0.426	0.431	0.426	0.967	0.977	0.995	1.000	2.23	2.23	-3.78	0.232
Shen	0.545	0.546	0.589	0.587	0.890	0.914	0.989	0.993	-21.47	-19.47	-15.47	-13.47
TM1	0.521	0.517	0.540	0.534	0.938	0.952	0.998	0.999	-10.87	-10.88	-0.88	-2.88
TMa	0.561	0.559	0.574	0.569	0.959	0.973	0.999	1.000	-13.09	-13.09	0.90	-3.10

TABLE I: Maximal matches and expected frequency biases for numerical waveforms with the templates described above. The biases seem surprisingly large and merit further investigation. Broadband: match is computed for $f \in [1,\ 5]\,\mathrm{kHz}$, narrow-band: $f \in [f_0 - 0.15,\ f_0 + 0.15]\,\mathrm{kHz}$, where f_0 is that which yields the maximum match in the broad frequency band.

where the inner product $(a|b)$ is defined:

$$(a|b) = \int_{f_{\min}}^{f_{\max}} \frac{\tilde{a}(f)\tilde{b}^*(f)}{S(f)}\ \mathrm{d}f. \tag{7}$$

Note the explicit presence of the frequency range used for the overlap calculation. Our principle interest is in measuring the dominant post-merger oscillation. We will, therefore, consider the 'broad-band' match over $[1,\ 5]\,\mathrm{kHz}$ which tells us how much of the total SNR in the signal we obtain with no knowledge of exactly where f_2 lies. Then, when we have found the frequency which yields the maximum overlap, we will restrict the match calculation to a narrow range around that frequency in order to determine how much SNR we can accumulate from that dominant oscillation using our simple templates.

Finally, we also study the expected bias in the frequency recovery using these tempates for a variety of post-merger signals. For the stationary-frequency waveforms (ring-down and gauss-down) we define the bias as,

$$\mathrm{bias} = f_2 - f_0. \tag{8}$$

For simplicity, I will just define the bias for the chirping waveforms as,

$$\mathrm{bias} = f_2 - f_p, \tag{9}$$

where f_p is the frequency of the peak of the power spectrum of the chirping waveforms. I still need to check how to get to f_p from the parameters of the chirping waveforms (critical for the Bayesian implementation later). This approach should work fine for studying the performance of our templates.

III. IMPLEMENTATION WITH BAYESIAN PARAMETER ESTIMATION

We now have a prototype code in place which will perform a parallel-tempering MCMC using any of the waveforms described in the previous section. So far, I have only produced preliminary resuls for the DD2 waveform, using the Gauss-down templates. The algorithm takes a few hours to run on a single injection, but I believe this can be improved enormously with some more careful tuning of the MCMC parameters (e.g., burn-in time, number of 'walkers', number of samples).

The output are samples from the joint-posterior PDF on the waveform parameters $\vec{\theta} = (A_0,\ f_0,\ t_0,\ \tau,\ \phi_0)$. For now, at least, we will only study the marginal posterior on f_0:

$$p(f_0|D) = \int_{\Psi} p(f_0, \vec{\psi}|M) p(D|f_0, \vec{\psi}, M)\ \mathrm{d}\vec{\psi}, \tag{10}$$

where $\vec{\phi} = (A,\ t_0,\ \tau,\ \phi_0)$. Again, please note that we are assuming an optimally oriented source and that we know the orientation with respect to the detector. The parameter space of the analysis will increase significantly if we use multiple detectors and relax that constraint[1].

Note that we place a Gaussian prior with $\sigma = 10\,\mathrm{ms}$ on the start time of the signal, taken to be the peak-time of the inspiral. Note also that we let the MCMC search for $f_0 \in [1.5,\ 4]\,\mathrm{kHz}$ and a data bandwidth of $[1,\ 5]\,\mathrm{kHz}$, to accommodate the finite extent of signals with f_0 at the boundaries. Again, this is somewhat wider to what we had before and we can easily restrict it. It's just interesting to study the most conservative range possible to begin with.

A particularly useful feature of parallel tempering, in addition to robustly sampling the posterior, is the computation of the Bayesian *evidence* or global likelihood of a model M,

$$p(D|M) = \int_{\Theta} p(\vec{\theta}|M)p(D|\vec{\theta}, M)\ \mathrm{d}\vec{\theta}. \tag{11}$$

We can then form the posterior odds ratio for a signal model S versus a noise model N:

$$\mathcal{O}_{S,N} = \frac{p(S|D)}{p(N|D)} = \frac{p(S)}{p(N)}\frac{p(D|S)}{p(D|N)}. \tag{12}$$

which tells us the relative probability of signal vs noise. While our principle concern here is the measurement of f_2, as opposed to detection at some level of confidence, we shall see that the posterior odds can be used to increase the robustness of the frequency estimation. Finally, it's common to set the prior odds (the first term in equation 12) to unity, which leaves us with the evidence ratio or *Bayes factor*:

$$B_{S,N} = \frac{p(D|S)}{p(D|N)}. \tag{13}$$

A. Frequency Recovery

Figure 1 shows ensembles of the measured frequency posterior $p(f_0|D)$ measured at 5, 10, 15 and 20 Mpc. Everything behaves exactly as we'd like it to and, indeed, we do appear *capable of identifying the correct frequency out to 20 Mpc.* Averaging over the sky, and assuming a 3-detector network with optimal combination of data streams (which is trivial in this framework), this is a sky-averaged distance of 15 Mpc. The figures which follow attempt to quantify these results.

[1] for a single-detector analysis, of course, all of the extrinsic sky-parameters are degenerate with the overall amplitude scale A

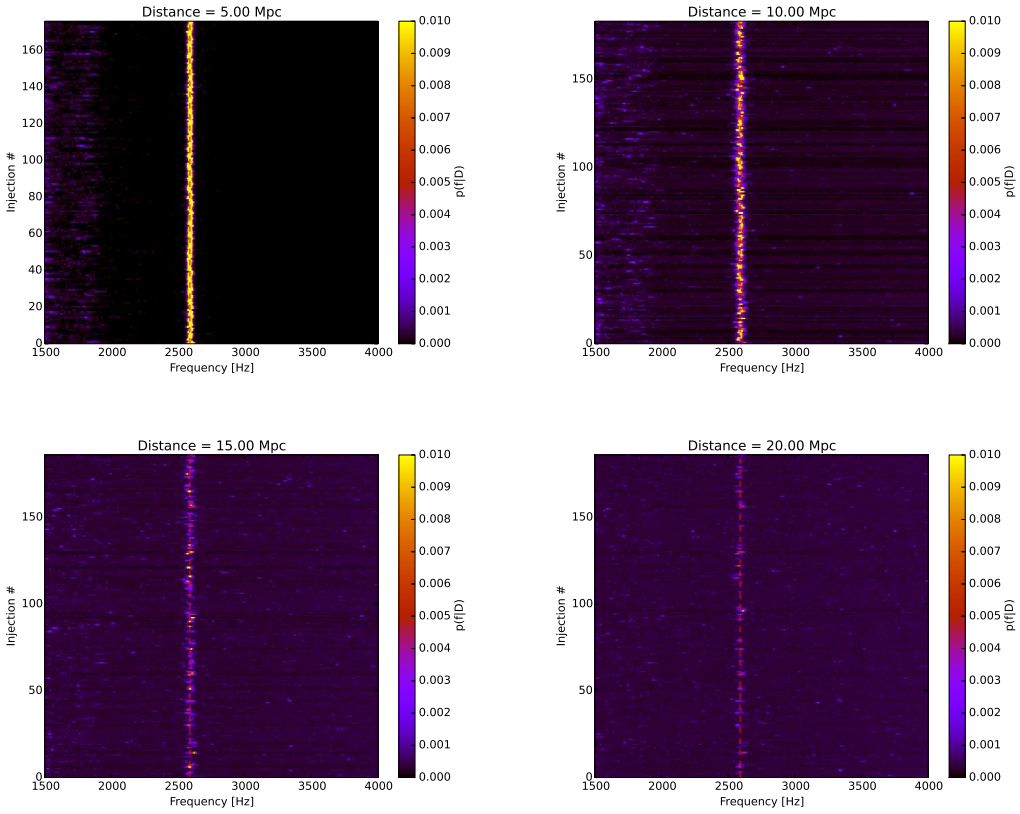

FIG. 1: Frequency posterior PDFs using a single detector for optimally oriented injections at 5, 10, 15 and 20 Mpc. The y-axis, 'injection number', corresponds to a different noise realisation in each case. These are all from the DD2 EOS. For nearby injections, the posteriors are sharply peaked (bright yellow) around the f_2 for DD2 (zoom in to see a red dashed line indicating f_2), and zero away from the peak (black surface). Quieter injections produce a nearly uniform frequency posterior (purple surface) with a small, but well-defined peak at the desired value (pink to yellow blobs, embedded in the purple background). Note that the louder signals also pick up some probability from the lower-frequency content. In our last paper, we placed lower bounds on f_2 which would restrict our prior well above this region. Here, I'm just being conservative and I'm curious to see what happens if we search for $f_2 \in [1.5,\ 4]\,\mathrm{kHz}$.

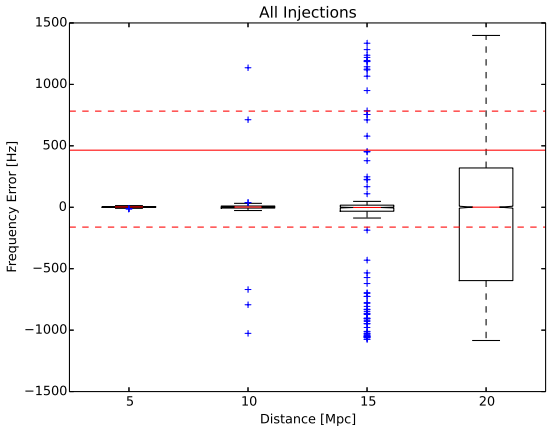

(a) Box-plot of the error in the estimated frequency using the Gauss-down template and taking the maximum of the marginal posterior on frequency as the point estimate. The boxes show the interquartile range, the red lines in the boxes are the median values and the whiskers show 1.5× the interquartile range. For reference, we also show as red horizontal lines the result one would expect to get by 'guessing': this is the result we should expect if we made no measurement at all and simply estimated the peak frequency from our prior; the solid horizontal red line is the median value of the frequency prior and the dashed horizontal red lines show the interquartile range. We therefore confirm that the measurement of the sources at 20 Mpc are indeed significantly better than simply guessing.

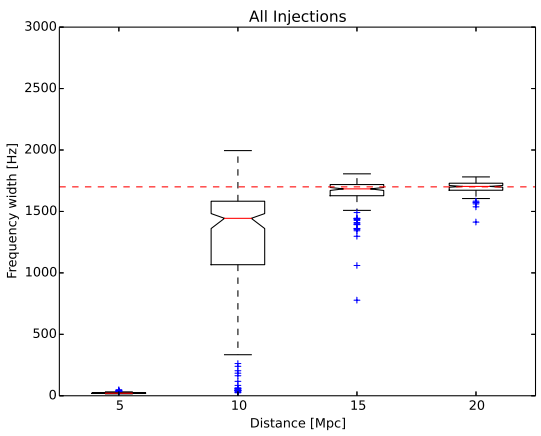

(b) Box-plot of the 68% confidence interval about the maximum of the frequency using the Gauss-down template and taking the maximum of the marginal posterior on frequency as the point estimate. Symbols have the same meaning as before. We now see that the confidence interval for the frequency estimate is extremely wide for quiet signals (as expected) and consistent with the uncertainty in the measurement one would get from 'guessing'. This does *not* mean we cannot measure the peak frequency at large distance; it simply means that the uncertainty in the measurement is large but we can have some confidence in its *accuracy* from the first panel.

FIG. 2: Frequency recovery assuming signal is present.

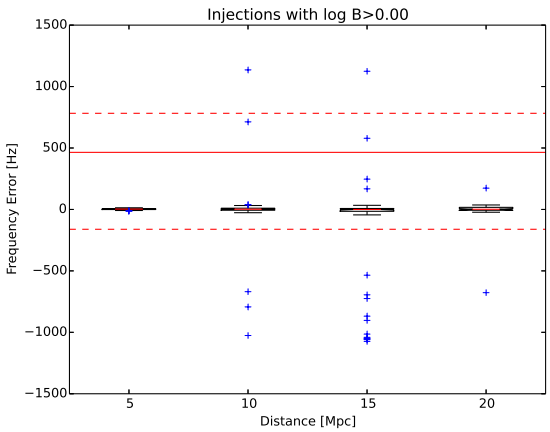

(a) As figure 2a but with the constraint that the posterior odds ratio (Bayes factor) is greater than unity (i.e., there's a better than 50/50 chance there's a signal there). We see that this dramatically improves the accuracy of the frequency measurement.

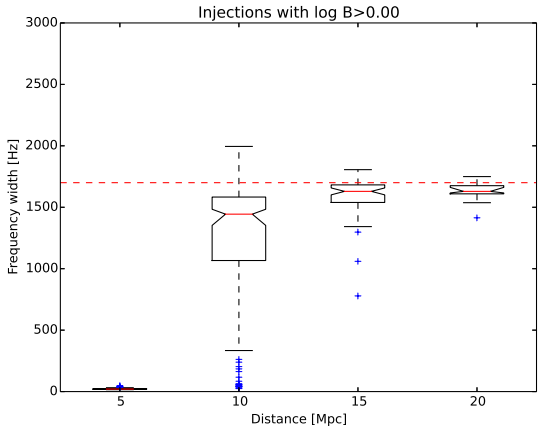

(b) Again, as figure 2b with the constraint that $\log B_{S,N} > 0$ (better than 50/50 odds of signal vs noise). This time, we see remarkably little change from the previous figure with no constraint. Given that the point estimate of the frequency at large distance with the constraint is so closely clustered around zero error, it is surprising that the posterior width is so large. This may point to a trivial code bug or problems in the kernel density estimation used to smooth the posteriors - I don't yet believe this result.

FIG. 3: Frequency recovery with the constraint that there is a better than 50/50 chance we think there's a signal there.

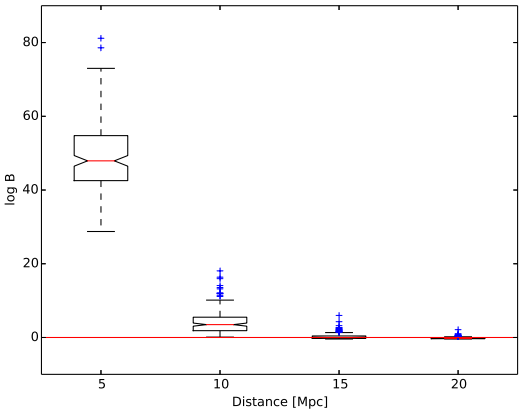

(a) The distribution of Bayes factors at different distances. By 20 Mpc there is little evidence for the presence of a signal and we basically have to get lucky.

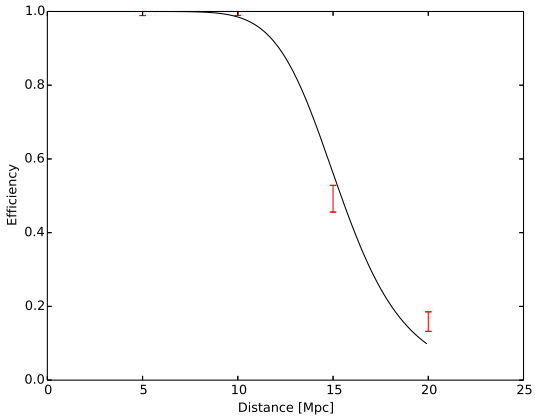

(b) The 'efficiency' (fraction of signals which produce $\log B_{S,N} > 0$ as a function of distance. The black curve is a sigmoid fit. More data is clearly needed, but we can see that by 20 Mpc, only about 18% of signals produce any evidence for their presence. However, as we have seen, those 18% do seem to have very accurate (if seemingly uncertain) frequency measurements.

FIG. 4: Behavior of and impact of the Bayes factor constraint $\log B_{S,N} > 0$.